

1 Dynamic range models improve the near-term forecast for a
2 marine species on the move

3 Alexa L. Fredston^{1,2*}, Daniel Ovando^{3*}, Lucas da Cunha Godoy⁴,
4 Jude Kong⁵, Brandon Muffley⁶, James T. Thorson⁷, Malin L. Pinsky^{4,2}

4 April 2026

5 *Co-first authors

6 ¹ Department of Ocean Sciences, University of California, Santa Cruz, fredston@ucsc.edu

7 ² Department of Ecology, Evolution, and Natural Resources, Rutgers University

8 ³ Inter-American Tropical Tuna Commission, dovando@iattc.org

9 ⁴ Department of Ecology and Evolutionary Biology, University of California Santa Cruz,
10 mpinsky@ucsc.edu

11 ⁵ Dalla Lana School of Public Health, University of Toronto, jude.kong@utoronto.ca

12 ⁶ Mid-Atlantic Fishery Management Council, bmuffley@mafmc.org

13 ⁷ National Oceanic and Atmospheric Administration, james.thorson@noaa.gov

14
15 **Running title:** Mechanistic models predict fish range shifts

16
17 **Keywords:** ecological forecasting, mechanistic modeling, species distribution, species redistribu-
18 tion, Bayesian hierarchical model

19
20 **Corresponding author:** Alexa Fredston, 1156 High St, Earth & Marine Sciences Bldg A455, Santa
21 Cruz, CA 95064. Phone: 831-459-2563. Fax: 831-459-4882. E-mail: fredston@ucsc.edu.

Abstract

23

24 Population dynamic models are widely used to predict demography. However, they have rarely
25 been extended to biogeographical applications despite widespread calls to do so. We developed
26 a process-based dynamic range model (DRM) that estimated demographic rates and the effects of
27 the environment on demographic rates to forecast species range shifts in response to temperature
28 change. As a proof of concept, we fitted DRMs to historical observations of summer flounder
29 (*Paralichthys dentatus*), a fish species in the Northwest Atlantic, and evaluated model skill at
30 retrospective forecasting. The best DRMs outperformed a statistical species distribution model
31 and a persistence forecast at predicting biogeographical dynamics across a decade. The DRM
32 approach is general and can be applied to a wide range of species with historical observations
33 across space and time. By explicitly modeling demographic processes and their relationship to
34 climate, DRMs promise to substantially advance prediction of species on the move.

Introduction

35

36 Prediction has become a central goal of ecology (Mouquet et al., 2015). Predictive ecology often
37 seeks to forecast human impacts on ecosystems. It supports biodiversity conservation, natural
38 resource management, climate change mitigation and adaptation, and other applications (Urban
39 et al., 2016). Near-term forecasting is a particularly pressing need so that the timescale of ecolog-
40 ical information aligns with the often-short timescale of environmental decision-making (Dietze
41 et al., 2018).

42 Species distributions have been a major emphasis of predictive ecology, particularly in the
43 context of climate change (Pearson & Dawson, 2003). Species are shifting their ranges in response
44 to climate change (Parmesan & Yohe, 2003), with cascading effects on communities, ecosystems,
45 ecosystem services, and human welfare and well-being (Pecl et al., 2017). Early species dis-
46 tribution models (SDMs) projected species ranges and range shifts using correlations between
47 species' presence (or sometimes abundance) and environmental variables (Elith & Leathwick,
48 2009). However, observed range shifts have been highly individualistic and are not well pre-
49 dicted by simple environmental variables (Davis et al., 1998; Rubenstein et al., 2023). SDMs have
50 been critiqued in the context of near-term forecasting because they assume species are in equilib-
51 rium with the environment, may be trained on data that does not resemble future climates, and
52 have demonstrated limited forecast skill to date (Jarnevich et al., 2015; Lee-Yaw et al., 2022). New
53 approaches (e.g., hybrid and ensemble SDMs) are addressing some of these shortcomings, but
54 still using fundamentally correlative approaches that do not explicitly model ecological mecha-
55 nisms (Brodie et al., 2022; Ehrlén & Morris, 2015; Kearney & Porter, 2009; Zurell, 2017).

56 Mechanistic or “process-based” models are often presented as a way forward in forecasting
57 range shifts and for predictive ecology in general (Dietze et al., 2018; Urban et al., 2016). These
58 models can estimate assumed causal relationships, predict effects using those estimates, provide
59 insight into fundamental ecological mechanisms, estimate parameters of interest, falsify ecologi-
60 cal hypotheses, and incorporate processes over varying spatial and temporal scales (Cabral et al.,
61 2017; Evans et al., 2016). Another advantage of mechanistic models is that (if implemented in a

62 hierarchical framework) they can model the underlying ecological processes separately from the
63 data collection process, facilitating more accurate parameter estimation and error partitioning
64 (Laubmeier et al., 2020). These are rare in biogeography, however, partly due to the heightened
65 difficulty of parameter estimation and scale when mechanistic ecological models (e.g., population
66 dynamic models) are made spatial (Briscoe et al., 2019).

67 One promising class of mechanistic models for range forecasting is dynamic range mod-
68 els (DRMs): spatially explicit population dynamic models that estimate demographic rates as a
69 function of the environment (Pagel & Schurr, 2012). DRMs estimate key parameters from data
70 on species' occurrences and abundances and can incorporate processes at multiple spatial and
71 temporal scales, making them flexible tools that may be applied to a broad suite of ecological
72 questions. However, this flexibility also makes them reliant on the availability of large datasets
73 through time and space. Indeed, DRMs have mainly been fitted to simulated data for this reason
74 (Zurell et al., 2016). DRMs have yielded useful results when applied to real data for parameter in-
75 ference (Le Squin et al., 2021; Osada et al., 2019). However, DRMs have not been operationalized
76 for range forecasting of real species—the main purpose for which they were designed (Briscoe
77 et al., 2019; Pagel & Schurr, 2012).

78 An ideal system in which to operationalize DRMs for range forecasting is one where species
79 have already shifted their ranges, where large-scale biodiversity surveys have been operating for
80 some time, and where a strong theoretical understanding exists of the underlying population
81 dynamics and how they relate to the environment. One such system is temperate marine con-
82 tinental shelf ecosystems. Range shifts have been particularly rapid and widespread in these
83 systems because there are relatively few barriers to dispersal, species live close to their ther-
84 mal limits, and spatial gradients in temperature are weaker in the oceans than they are on land
85 (Pinsky et al., 2020). Marine systems are also relatively data-rich: we have records of historical
86 fishing mortality, insights into the population dynamics of harvested marine species, and large-
87 scale, long-term monitoring programs that have conducted scientific marine surveys for many
88 decades (Maureaud et al., 2023).

89 Here, we built DRMs—mechanistic models that explicitly model demographic processes from

90 physiological to metapopulation scales—to forecast range dynamics in response to climate vari-
91 ability and change using more than four decades of biogeographical data. We implemented these
92 DRMs as hierarchical Bayesian models fitted to historical data from 1972-2006 on summer floun-
93 der (*Paralichthys dentatus*), an important commercial and recreational fishery species on the east
94 coast of the US. Harvest and management of summer flounder have been controversial in this
95 region for decades (Terceiro, 2011), even before recent evidence that the stock has been shifting
96 northward (Perretti & Thorson, 2019); thus, understanding patterns and trends in this species’
97 spatiotemporal abundance in light of warming temperatures is also a priority for regional fishery
98 managers and stakeholders. We then evaluated DRM performance with a retrospective forecast
99 from 2007-2016. We modeled the data collection process separately from the underlying ecologi-
100 cal dynamics and quantified both process and measurement error. We designed multiple DRMs
101 representing different hypotheses about the underlying ecological processes; this allowed us to
102 explore which vital rates were most strongly affected by changing temperatures and the value
103 of incorporating additional ecological complexity (Briscoe et al., 2019; Zurell et al., 2016). Specif-
104 ically, we compared DRMs with temperature-dependent recruitment, mortality, or movement.
105 Out-of-sample DRM forecasts were more accurate and less biased than a statistical SDM or a
106 persistence forecast at predicting range centroid and edge positions over a decade of testing.

107 **1 Methods**

108 We aimed to develop a DRM configuration that balanced broad applicability across species and
109 ecosystems with relevance to our focal species. The DRM simulated age-structured, discrete-
110 time population dynamics that are generally applicable to many species. For summer flounder,
111 we then grouped the ages into three life stages (recruits, juveniles, and adults) to capture key
112 ontogenetic differences in its life history (see Section 1.1.1) without estimating a large number
113 of age-specific parameters for this relatively long-lived species. The number of stages and the
114 relationship between age and stage structure could easily be changed in future applications of
115 the DRM to other taxa and systems.

116 We discretized the spatial domain of the DRM into 10 habitat patches of 1° latitude along the

117 coastline (Fig. 2) such that each patch was adjacent to one or two neighboring patches (Fig. 1). We
118 made this choice to introduce sufficient spatial structure that the model could reproduce changes
119 in the species' range while not trying to fully resolve dispersal at such high resolutions over
120 space and time that the model would be computationally intractable or contain non-identifiable
121 parameters. We did not attempt to tailor the patch structure to summer flounder-specific biogeo-
122 graphic details and instead chose a generic spatial structure such as would be required for most
123 species lacking such information. We also note that nothing about the DRM requires patches to
124 be adjacent, and future applications of the DRM could add more complex patch structures and
125 dispersal matrices to represent long-distance dispersal, oceanographic currents, or biogeographic
126 breaks (Pappalardo et al., 2015; Watson et al., 2010). Summer flounder larvae disperse widely
127 and without clear directionality despite prevailing southward ocean currents in the region (Hoey
128 & Pinsky, 2018; Hoey et al., 2020) and adults are relatively mobile (Lux & Nichy, 1981). We
129 therefore assumed that recruitment was a global process that did not vary over space (see Equa-
130 tion (1)) unless temperature effects were introduced (see Section 1.1.2); that juveniles could not
131 move; and that adults moved between adjacent patches (see Equation (5)). These assumptions
132 reflect a common scenario for marine animals: a well-mixed regional larval pool, low-mobility
133 juveniles, and highly mobile adults. Each of these assumptions can be easily modified in future
134 DRM implementations, including by adapting Equation (1) to estimate patch-specific recruitment
135 or density dependence (e.g., Pagel & Schurr, 2012), or to allow movement at different ages.

136 Model parameters were estimated by fitting this process-based model to observations of
137 species abundance density across space and time. We implemented a base model without
138 temperature-dependent demographic rates and three models with temperature-dependent re-
139 cruitment, mortality, or movement. We denote vectors, matrices, and arrays in bold. We used a
140 hierarchical Bayesian approach to model observed numerical densities of all individuals regard-
141 less of age (\mathbf{D}) as a function of the modeled latent age-structured population density ($N_{p,a,t}$) for
142 each patch (p), age class (a), and time step (t). In our implementation, the units of both a and t
143 were in years, i.e., one time step was one year. We incorporated observed presence (\mathbf{P}) to help
144 account for zero-density patches. Our methodology comprises a process model, which explicitly

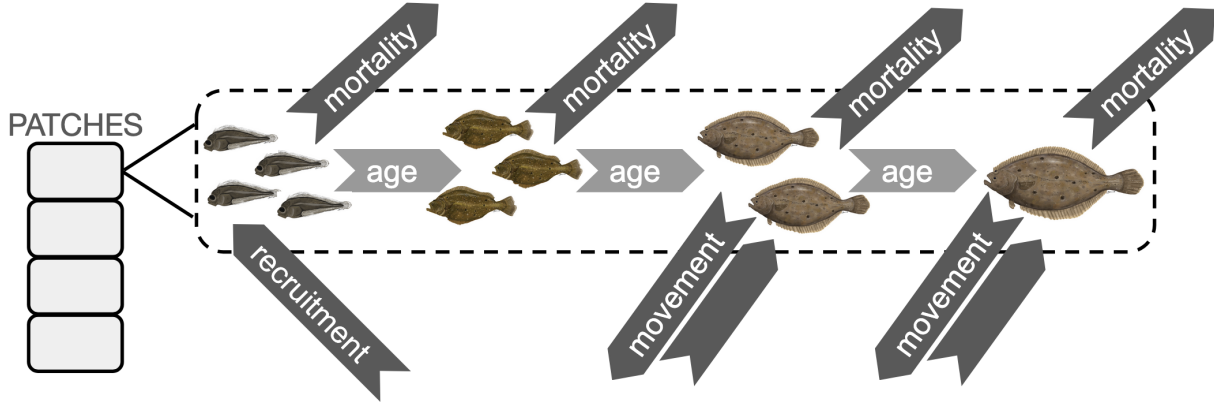


Figure 1: Schematic of the patch structure and temperature-dependent processes in the DRM design highlighting dynamics within an example patch. All patches contained distinct age classes and experienced stochastic recruitment. The three processes for which a temperature effect could be implemented are shown as dark grey arrows. Temperature-dependent recruitment affected the production of recruits by adults; temperature-dependent mortality affected all age classes; and temperature-dependent movement affected the dispersal of adults between adjacent patches.

145 models the underlying population dynamics, and an observation model, which relates these dy-
 146 namics to observed data. We first describe the structure of the process model and its alternative
 147 configurations, followed by the observation model, which remained consistent across all process
 148 model configurations.

1.1 Process models

1.1.1 Base model

151 The base process model included age structure, adult dispersal, stochastic recruitment, and an-
 152 nual mortality for fifteen ages to match summer flounder life history in the northeast U.S. Ap-
 153 plication to shorter- or longer-lived organisms would consider fewer or additional age classes.
 154 The population dynamics driving $N_{p,a,t}$ were as follows. Recruitment (i.e., production of age 1
 155 individuals) in each year and patch was calculated as a stochastic process (Johnson et al., 2016)
 156 around a long-term average:

$$N_{p,a=1,t} = \mu \times e^{rt - \frac{\sigma_{\text{proc}}^2}{2}} \quad (1)$$

157 where μ is the average density of recruitment per patch across all space and time, r_t represents
 158 recruitment stochasticity (through a first-order autoregressive process), and σ_{proc} is its condi-
 159 tional standard deviation. Equation (1) implies that recruitment in a given year is the same
 160 for all patches. Fertilized summer flounder larvae spend approximately a month in a pelagic
 161 phase during which they are broadly transported by currents (Keefe & Able, 1993). The species
 162 is considered to have a single, well-mixed population in the study region and has little rela-
 163 tionship between adult biomass and annual recruitment (NEFSC, 2019), which motivated our
 164 representation of recruitment as a region-wide, density-independent process. Substantial larval
 165 dispersal and interannual variation in recruitment is common across marine fishes and inverte-
 166 brates (Houde, 2008). Application to other kinds of species could modify this equation to instead
 167 consider local density dependence or eliminate the stochastic component (e.g., Pagel & Schurr,
 168 2012).

169 The autoregressive term r_t was defined as

$$r_t = \alpha r_{t-1} + \sigma_{\text{proc}} z_t, \quad (2)$$

170 where z_t is an uncorrelated standard Normal error term and α is the temporal autocorrelation,
 171 namely the correlation between r_t and r_{t-1} .

172 We modeled adults and juveniles (the latter are older than recruits but not yet mobile or
 173 reproductive) separately. Summer flounder reach maturity around two years of age (NEFSC,
 174 2019), so in our implementation, age class one represented recruits, age class two represented
 175 juveniles, and age classes three and older represented adults. Juvenile age classes were modeled
 176 as the fraction of the younger age class that survived to the following year in a given patch:

$$N_{p,a=2,t} = N_{p,a-1,t-1} \times s_{a-1,t-1} \quad (3)$$

177 where s represents annual survival fraction, which was constant across patches in the base model.
 178 Because summer flounder experience fishing mortality, we combined age- and year-specific fish-
 179 ing mortality $f_{a,t}$ with natural mortality m to calculate the annual survival fraction:

$$s_{a,t} = e^{-(f_{a,t}+m)}. \quad (4)$$

180 Both m and $f_{a,t}$ are instantaneous rates, so they can exceed 1. The fishing mortality term would
 181 be removed for species that are not harvested by humans. More complicated applications could
 182 consider adding predator or other sources of mortality in this equation.

183 Adult summer flounder are highly mobile predators that migrate offshore seasonally, so
 184 adults in the model differed from juveniles in that they could move among adjacent patches.
 185 In this base model, we calculated age-structured population density for adults with an isotropic
 186 dispersal fraction δ among adjacent patches:

$$\begin{aligned} N_{p,a,t} = & (1 - 2\delta)N_{p,a-1,t-1} \times s_{a-1,t-1} \\ & + \delta N_{p-1,a-1,t-1} \times s_{a-1,t-1} \\ & + \delta N_{p+1,a-1,t-1} \times s_{a-1,t-1}, \text{ for } a > 2. \end{aligned} \quad (5)$$

187 Edges were treated as reflective for adults so that they did not disperse beyond the model domain,
 188 and dispersal rates were adjusted accordingly at the edges. Therefore, we specified $N_{p,a,t} =$
 189 $(1 - \delta)N_{p,a-1,t-1} \times s_{a-1,t-1} + \delta N_{p-1,a-1,t-1} \times s_{a-1,t-1}$ in the northern-most patch, and $N_{p,a,t} =$
 190 $(1 - \delta)N_{p,a-1,t-1} \times s_{a-1,t-1} + \delta N_{p+1,a-1,t-1} \times s_{a-1,t-1}$ in the southern-most patch, for $a > 2$. This
 191 assumption matches the active movement choices that adult summer flounder make. For species
 192 with dispersal at different ages or in different fashions, these decisions could be easily adapted.

193 1.1.2 *Temperature effects*

194 To incorporate the effects of temperature on demographic processes—and, consequently, on
 195 species distributions over space and time—we designed a series of alternative models for tem-
 196 perature dependence. These demographic impacts are not known for summer flounder, just as
 197 they remain unknown for most species on Earth, and so the DRM inferred which parameters best
 198 matched the spatiotemporal patterns of species abundance. These models represented different
 199 hypotheses describing how temperature may affect population dynamics. For example, adults

200 might move to track their preferred thermal conditions, and indeed, marine species ranges are
 201 highly correlated with their physiological thermal tolerances (Sunday et al., 2012). Adult move-
 202 ments in summer flounder are also seasonal (Packer et al., 1999), which could plausibly be linked
 203 to temperature. In addition, the distribution of recruits has shifted north faster than adults for
 204 some species, suggesting that temperature might instead affect recruitment (Perretti & Thorson,
 205 2019). Lab studies and historical population dynamics in summer flounder are consistent with
 206 temperature effects on natural mortality (O’Leary et al., 2019; Packer et al., 1999), and temper-
 207 ature effects on mortality are quite general across species (Munch & Salinas, 2009). To explore
 208 these three hypotheses in the context of range shifts, we implemented alternative models that
 209 included temperature effects on (1) recruitment, (2) mortality, or (3) adult movement. To avoid
 210 parameter identifiability issues, we tested these temperature effects in separate models while
 211 acknowledging that all three could operate simultaneously to some extent. Climate effects on
 212 reproduction, survival, and movement are thought to be widespread (Scheffers et al., 2016), and
 213 so we expect that these models will be widely useful across other species as well.

214 In each case, we calculated a relative index of temperature suitability for each patch and year,
 215 I . I was maximized at an optimal temperature, τ , which was estimated as part of model fitting.
 216 Although it always represented an optimal temperature in °C, the biological interpretation of τ
 217 depended on the model structure. In the recruitment model, τ was the temperature at which
 218 recruitment was highest. In the mortality model, it represented the temperature at which nat-
 219 ural mortality was at its baseline level. In the movement model, τ represented the temperature
 220 toward which the greatest proportion of fish migrated from an adjacent patch. In all cases, I was
 221 calculated as a Gaussian function such that, as the actual temperature T deviated from τ , the
 222 temperature suitability index I declined at a rate inversely proportional to a width parameter ω
 223 that was also estimated,

$$I_{p,t} = e^{\left(-0.5\left(\frac{T_{p,t}-\tau}{\omega}\right)^2\right)}. \quad (6)$$

224 The temperature-dependent recruitment model linked patch-specific temperature to recruit-
 225 ment by using I to rescale $N_{p,a=1,t}$, thus modifying Equation (1):

$$N_{p,a=1,t} = \mu \times e^{r_t - \frac{\sigma_{\text{proc}}^2}{2}} \times I_{p,t}. \quad (7)$$

226 In this case, μ becomes the average density of recruits under optimal environmental conditions,
 227 that is, when $T = \tau$. For application to other species, researchers could consider environmental
 228 factors other than temperature, or, where relevant, modify the equation so that recruitment is
 229 influenced by environmental conditions in a distant spawning or mating location, rather than
 230 where the offspring recruit.

231 To model temperature-dependent mortality, we modified Equation (4) to include the temper-
 232 ature effect \mathbf{I} , which acted by reducing survival when the temperature was not at τ :

$$s_{p,a,t} = e^{-(f_{a,t} + m + \gamma(1 - I_{p,t}))}, \quad (8)$$

233 where γ scales the excess natural mortality due to temperature. Note that, unlike in Equation (4),
 234 s could now vary over p because the temperature effect led to distinct survival across patches.
 235 This formulation allowed mortality to increase at low or high temperatures, if such processes
 236 helped explain the spatiotemporal abundance data. More generally across species, mortality
 237 is often modeled as an increasing exponential function of temperature through a Boltzmann-
 238 Arrhenius function (McCoy & Gillooly, 2008).

239 The movement model required more complexity because we modeled both passive diffusion
 240 between patches and taxis—the directed movement by adults in response to environmental gra-
 241 dients. Such movement models are quite general and are widely used across animal ecology
 242 (J. R. Potts & Schlägel, 2020; Preisler et al., 2013), though even more complex movement models
 243 that consider individual decisions and biophysical interactions are also available (Morales et al.,
 244 2010; Swearer et al., 2019). We followed the diffusion-taxis methods in Thorson *et al.* (2021).
 245 Specifically, we log-transformed \mathbf{I} and constructed a p -by- p taxis matrix \mathbf{X} for each year by sub-
 246 tracting the \mathbf{I} of adjacent patches and multiplying the difference (i.e., the habitat gradient) by
 247 β_{tax} , a parameter that defined how much taxis changed per unit of temperature. A p -by- p dif-
 248 fusion matrix, \mathbf{Z} , simply included δ for adjacent patches (rescaled so that columns in the matrix

249 summed to 1 at the end) and zeros elsewhere. We then summed and matrix exponentiated \mathbf{Z}
 250 and \mathbf{X} in every year to yield the annual transition matrix $\mathbf{M} = e^{\mathbf{X}+\mathbf{Z}}$ containing annual movement
 251 fractions between each patch. Although $\mathbf{X} + \mathbf{Z}$ is only nonzero for adjacent patches (i.e., instan-
 252 taneous taxis and diffusion only occurs locally), the annual transition matrix $\mathbf{M} = e^{\mathbf{X}+\mathbf{Z}}$ is dense
 253 (i.e., annualized movement can connect any two patches). Movement between non-adjacent cells
 254 is biologically plausible for mobile animals. Finally, we calculated abundance as

$$\mathbf{n}_{a,t}^T = \mathbf{n}_{a-1,t-1}^T \times s_{a-1,t-1} \mathbf{M}, \text{ for } a > 2 \quad (9)$$

255 where $\mathbf{n}_{a,t}^T$ is the row-vector of abundance $N_{p,a,t}$ across patches p , and this equation then replaced
 256 the previous Eq. 5.

257 1.2 Observation model

258 The observation model related the observed densities to the process model. We defined observed
 259 presence ($P_{p,t}$) from observed density ($D_{p,t}$) at patch p and time t as

$$P_{p,t} = \begin{cases} 1 & \text{if } D_{p,t} > 0 \\ 0 & \text{if } D_{p,t} = 0. \end{cases} \quad (10)$$

260 We assumed $P_{p,t}$ and $D_{p,t}$ were distributed as follows

$$P_{p,t} \sim \text{Bernoulli}(\theta_{p,t}) \quad (11)$$

$$(\log(D_{p,t}) | P_{p,t} = 1) \sim \mathcal{N} \left(\log(\lambda_{p,t}/\theta_{p,t}) - \frac{\sigma_{obs}^2}{2}, \sigma_{obs} \right), \quad (12)$$

261 where $\theta_{p,t}$ is the probability of encountering individuals in patch p and time t , \mathcal{N} indicates a
 262 Normal distribution, σ_{obs} is the standard deviation of $\log(D_{p,t})$, and $\lambda_{p,t}$ is the latent density of
 263 individuals in each patch expected to be observed by the survey. Note that we divided $\lambda_{p,t}$ by
 264 $\theta_{p,t}$ in Equation (12) to ensure that product of encounter probability $\theta_{p,t}$ and expected positive
 265 catch $\mathbb{E}[D_{p,t} | P_{p,t} = 1]$ is equal to to predicted density $\lambda_{p,t}$, i.e., $\mathbb{E}[D_{p,t}] = \lambda_{p,t}$.

266 A logit-link was used to connect the probabilities of encounter $\theta_{p,t}$ to the predicted densities
267 as follows

$$\text{logit}(\theta_{p,t}) = \beta_0 + \beta_1 \log(\lambda_{p,t}), \quad (13)$$

268 where β_0 and β_1 are slope and intercept parameters controlling how much the probability of
269 the species being encountered increases with the latent density. Our formulation is similar to
270 two-stage (or hurdle) models appropriate for many species observations across space and time
271 that contain large numbers of zeros (J. M. Potts & Elith, 2006).

272 The ability of the survey (see Section 1.4) to observe summer flounder individuals depended
273 on their size. To relate fish observations to the latent, age-structured densities in the DRM, we
274 converted density-at-age to density-at-length using a length-at-age relationship. This relationship
275 assumed that summer flounder, on average, grow according to a von Bertalanffy curve with log-
276 normal deviations and a constant coefficient of variation of 20%. Using this relationship, we
277 converted density of fish at a given age a to density of fish at length. From there, we assumed
278 that the survey gear had a logistic selectivity curve, with the lengths at 50% and 95% selectivity
279 estimated by the model. This selectivity curve converted the age-structured density of fish in the
280 model ($N_{p,a,t}$) to the expected density of fish caught by the survey ($\lambda_{p,t}$):

$$\lambda_{p,t} = \sum_a \Phi(a) N_{p,a,t} \quad (14)$$

281 with the function $\Phi(a)$ encoding the probability of sampling an individual of age a . For applica-
282 tion to other species or even the same species with other datasets, this part of the model would
283 likely change to reflect different observation processes.

284 1.3 Model implementation

285 We wrote the DRM in Stan, a platform for Bayesian modeling (Stan Development Team, 2021),
286 and used “cmdstanr” (Gabry et al., 2024) to produce the results in R (Supp. Tab. 1). We
287 specified weakly informative priors for parameters α , β_0 , β_1 , σ_{obs} , and δ . We also bounded them
288 to ecologically meaningful values: β_1 was restricted to positive numbers, and δ was restricted

289 to the interval $[0, 1/3]$. The prior for α was based on the recruitment autocorrelation estimated in
290 previous studies (Johnson et al., 2016; Thorson et al., 2014). We also specified weakly informative
291 priors for additional parameters in temperature-dependent models (Supp. Tab. 2). We specified
292 fishing $f_{a,t}$ and natural mortality rate m as known values and informed priors, respectively (see
293 Section 1.4).

294 For each model configuration, we obtained samples from the posterior from four parallel
295 chains, each of which ran for 5,000 iterations, including 2,000 warm-up iterations. We consid-
296 ered a model to have converged if less than 5% of the transitions in the sampler after warm-up
297 were reported as divergent. All statistical results from Bayesian models were reported with 95%
298 Highest Posterior Density Intervals (HPDI) using the “coda” package in R (REF).

299 1.4 Data

300 To fit and evaluate the DRMs, we used data from National Oceanic and Atmospheric Administra-
301 tion (NOAA) bottom trawl surveys conducted in the northeast US since 1968 (Smith, 2002). These
302 surveys have been conducted with standardized equipment and methods over time, and utilize
303 a stratified random sampling design, making them ideal for climate biogeography applications
304 (Fredston et al., 2021; Fredston-Hermann et al., 2020; Pinsky et al., 2013). We downloaded the
305 2020 release of OceanAdapt, a data portal that compiled North American bottom trawl survey
306 records (Forrest et al., 2020). The NOAA Northeast survey operates in fall and spring; we used
307 the fall survey that had more records of our focal species. To ensure that the years analyzed were
308 sampled consistently throughout time, we used data from 1972-2016; this interval began when
309 the surveys were standardized (Fredston et al., 2021; Fredston-Hermann et al., 2020; Pinsky et al.,
310 2013) and ended before data gaps caused by recent disruptions to survey funding and operations,
311 including the COVID-19 pandemic. These records encompassed the region from Cape Hatteras
312 in North Carolina to the border between Canada and Maine (Fig. 2), from just north of 35°N to
313 above 44°N.

314 The sampling unit for the survey is a single “haul”, an event during which a fishing net is
315 towed through the ocean for a fixed amount of time. Temperature is measured *in situ* for each

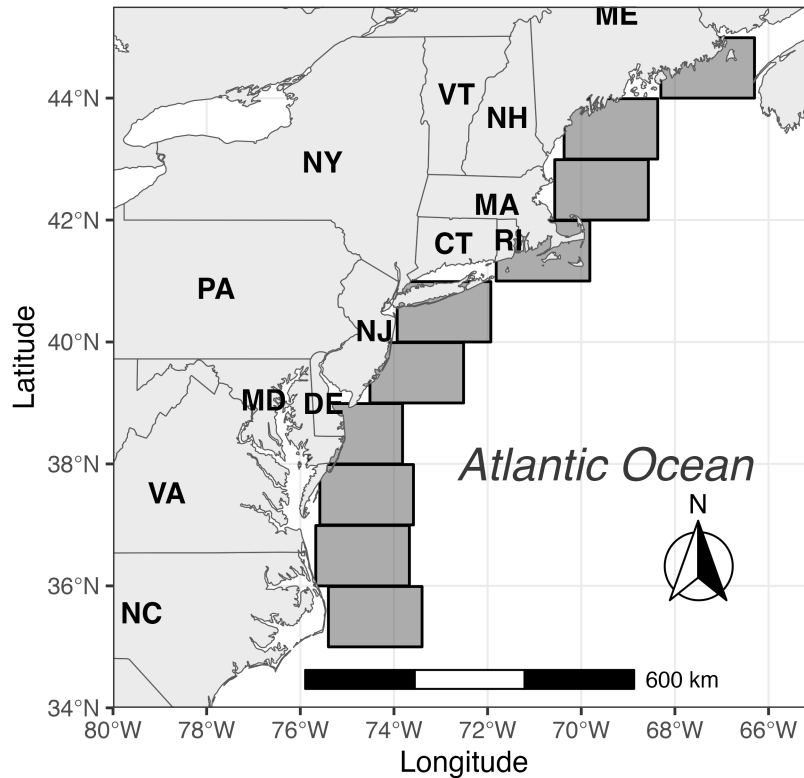


Figure 2: Map of the study region showing the modeled patches as grey boxes. Each patch was 1° latitude high. US states are labeled for reference.

316 haul at the seafloor. After each haul, scientists on board the survey vessel identify, count, weigh,
 317 and measure the catch in the net. We calculated $D_{p,t}$ as the average number of summer flounder
 318 per haul in patch p in year t . These observed density values—varying over space and time—were
 319 the main data input to the DRM.

320 We averaged bottom temperature data across hauls in every patch and year. *In situ* sea
 321 bottom temperature data was missing for some hauls, including all hauls south of 38°N in 2008.
 322 To fill this data gap, we fitted a Bayesian linear regression using Gaussian errors with latitude
 323 as a fixed effect, year as a group-level (random) effect with varying intercepts, and all available
 324 bottom temperature data as the response variable. We then used this fitted model to predict
 325 bottom temperature in patch-year combinations that were missing data.

326 Summer flounder are intensively fished (Terceiro, 2011), and so we leveraged existing sci-

327 entific information on their mortality caused by fishing and other factors (NEFSC, 2019). This
328 component of the DRM could be simplified in future applications where (unlike for summer
329 flounder) harvest is not important to population dynamics. Summer flounder have a stock as-
330 sessment, which is a statistical analysis that integrates many regional surveys of both fish and
331 fisheries catch, plus other information, to estimate fishery catch rates and other information that
332 guides fisheries management (NEFSC, 2019). The assessment estimated instantaneous fishing
333 mortality-at-age $f_{a,t}$, which varied across years t and age-classes a and ranged from 0.009 to 1.983
334 (NEFSC, 2019). We passed $f_{a,t}$ to the DRM as a parameter known without error. The assessment
335 estimates of f began in 1982, so we imputed the 1982 values for our earliest years of summer
336 flounder data (1972-1981). Based on summer flounder life history, the stock assessment assumed
337 that $m = 0.25$; we used this value as an informative prior to model m in each DRM configuration
338 (Supp. Tab. 2).

339 *1.5 Species distribution model*

340 To compare DRM performance to SDMs widely used in the range shift literature, we fitted a gen-
341 eralized additive model (GAM) SDM (Morley et al., 2018) with the “mgcv” package in R (Wood,
342 2017). The GAM SDM was a two-stage model; we fitted one GAM to presences and absences in
343 the training data using a logistic regression (i.e., logit-link and Bernoulli family) and a second
344 GAM to log-abundance conditioned on presence, assuming a Gaussian error distribution. Both
345 were single intercept models with a spline on bottom temperature, the sole predictor. Unlike
346 the DRMs, we fitted the GAM to the haul-level data (not aggregated to the patch scale). Bottom
347 temperature records were missing from a number of hauls in 2008 (see Section 1.4). The inter-
348 polation method we used to fill these data gaps for the DRMs was not appropriate for the much
349 higher spatial resolution of the GAMs, so we omitted 2008 data from the GAMs.

350 *1.6 Model evaluation and comparison*

351 We used a retrospective forecasting approach to assess model performance. The DRM and SDM
352 were fitted to summer flounder data from 1972-2006 and then simulated for the final decade of

353 data (2007-2016). The DRM forecast was initialized with the final year of fishing mortality data
354 passed to the model (2006) and then run forward by making draws from the posterior probability
355 distribution of parameters estimated in the model fitting routine. Observed temperature data for
356 2007-2016 were used. We validated the forecasts against the held-out observations from 2007-
357 2016, which we averaged into patches as we did for the input to the DRM (Section 1.4). The
358 GAM SDM forecast used the bottom temperature records from 2007-2016. We then aggregated
359 GAM predictions to the patch scale the same way we aggregated the raw data passed to the DRM
360 (Section 1.4) to enable forecast comparisons. We also evaluated a persistence forecast, which was
361 a continuation of the observations from the final year of the training interval (2006) into every
362 subsequent year.

363 Forecast performance metrics included (1) the abundance-weighted latitudinal range center
364 (i.e., range centroid) and (2) the cold and (3) the warm range edge positions. The edge positions
365 were calculated as abundance-weighted 0.05 and 0.95 quantiles of latitude (Fredston et al., 2021;
366 Fredston-Hermann et al., 2020). Note that because our study domain did not encompass the full
367 geographic distribution of the focal species (which is found at lower densities in the southeast
368 US as well), these represented population range metrics, not metrics for the full species range.

369 For each of these metrics, we calculated the residuals (forecasts minus observations) in each
370 year. We then calculated bias (mean of residuals) and root mean square error (RMSE, square root
371 of the mean of the squared residuals) for each metric. For the DRMs, we calculated the residuals
372 for each of 12,000 posterior draws and then used the mean residual value for each posterior to
373 calculate bias and RMSE.

374

2 Results

375 Summer flounder exhibited complex spatiotemporal dynamics during the study period, includ-
376 ing a decline in density in the 1980s and an increase beginning in the 1990s (Fig. 3). Its geographic
377 distribution was relatively stable from 1972-1990, then shifted north substantially through 2002
378 before another period of relative stability through 2016 (Fig. 3). During the northward shift
379 (1990-2002), for example, the centroid shifted from the latitude of Virginia (37.7 °N) to that of

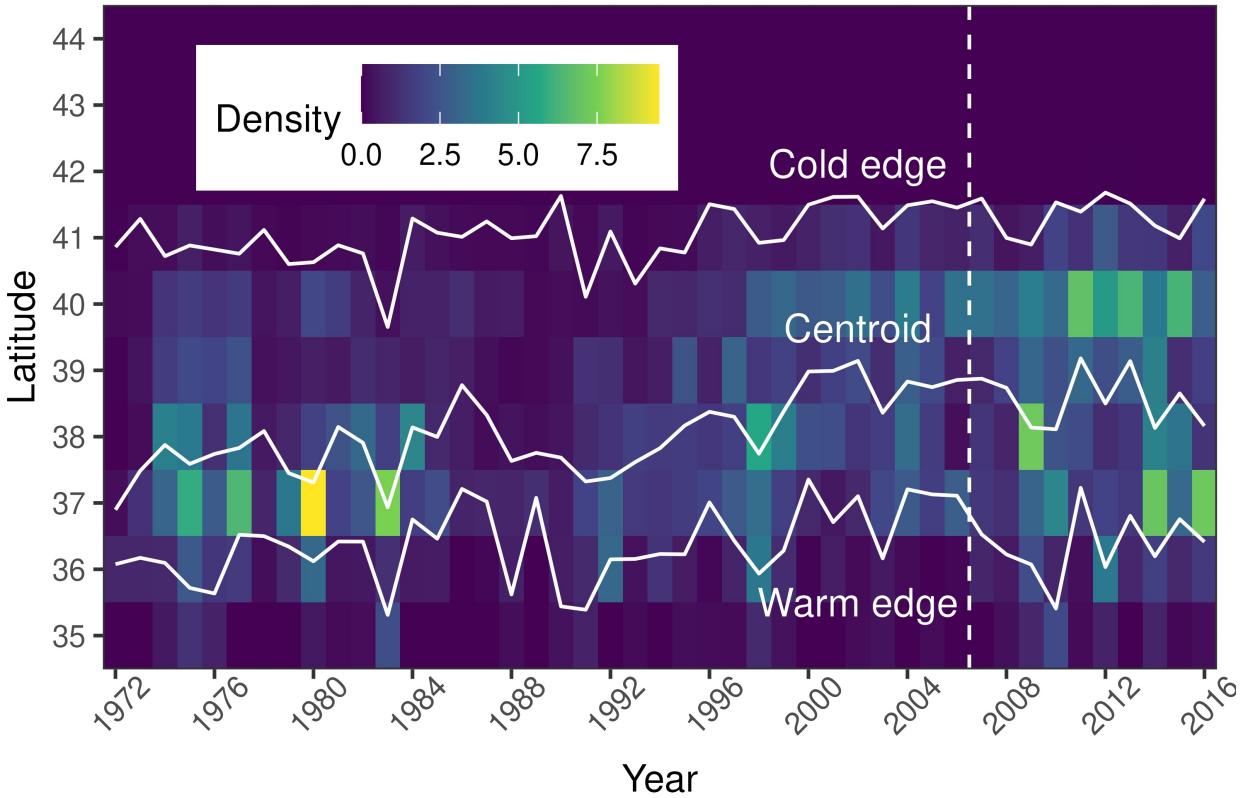


Figure 3: Observed summer flounder dynamics over space and time in the study region from 1972-2016. Cells are color-coded by mean density in the survey, and summary statistics used to evaluate and validate models (the position of the range centroid and warm and cold edges) are plotted.

380 New Jersey (39.1 °N), approximately 155 km (Fig. 2). These observed shifts occurred primarily
381 during our model training interval. From 2007-2016 (our testing interval), summer flounder did
382 not shift north significantly (Bayesian linear regression of latitude on time; 95% HPDI -0.15 –
383 0.09, -0.10 – 0.19, and -0.07 – 0.10 for the range centroid, warm edge, and cold edge, respectively;
384 Fig. 3).

385 The *in situ* sea bottom temperature exhibited warming of 0.04 °C per year across the study
386 region from 1972-2016 (median posterior value from Bayesian linear regression of temperature
387 on year; 95% HPDI 0.04 – 0.05). This trend was spatially and temporally heterogeneous; warming
388 was concentrated in the center of the study domain (Fig. 2) during the training period (Supp.
389 Tab. 3), with a particularly intense period of warming from 1988-2000 (Fig. 4) that aligned with
390 the strong northward shift observed in flounder (Fig. 3). During the testing decade, warming
391 was concentrated in the northern half of the study domain, starting at 40 °N (Fig. 4, Supp. Tab.
392 4).

393 Observations were available for 14,025 individual summer flounder caught across 12,203
394 hauls from 1972-2016. As is common in marine fish surveys, the data were heavily zero-inflated;
395 81% of these hauls did not catch any summer flounder and 96.5% of hauls caught fewer than ten
396 (Supp. Fig. 1). The number of hauls per year was generally between 225 and 325, although 1978
397 and 1979 had almost 500 (Supp. Fig. 2).

398 All four DRM configurations (no temperature effect, or temperature effect on recruitment,
399 mortality, or movement) converged when fit to the data and produced density estimates consis-
400 tent with observations (Supp. Fig. 3-6). The models generally reproduced the decline in density
401 until 1990 and the increase afterwards, though the null model (no temperature effect) failed
402 to re-create the lower abundances towards the northern and southern range edges and higher
403 abundance in mid-latitudes (Supp. Fig. 3). The DRMs with temperature-dependent demogra-
404 phy, and particularly recruitment or mortality, more effectively captured these spatial gradients
405 (Supp. Fig. 4-6). In addition, their parameter estimates differed substantially (Supp. Fig. 7).
406 Temperature-dependent recruitment had an optimum of 14.7 – 14.9 °C with a width of 1.49 –
407 1.60 °C (95% HPDI; see Eqn. 6), suggesting a narrow range of optimal temperatures for recruit-

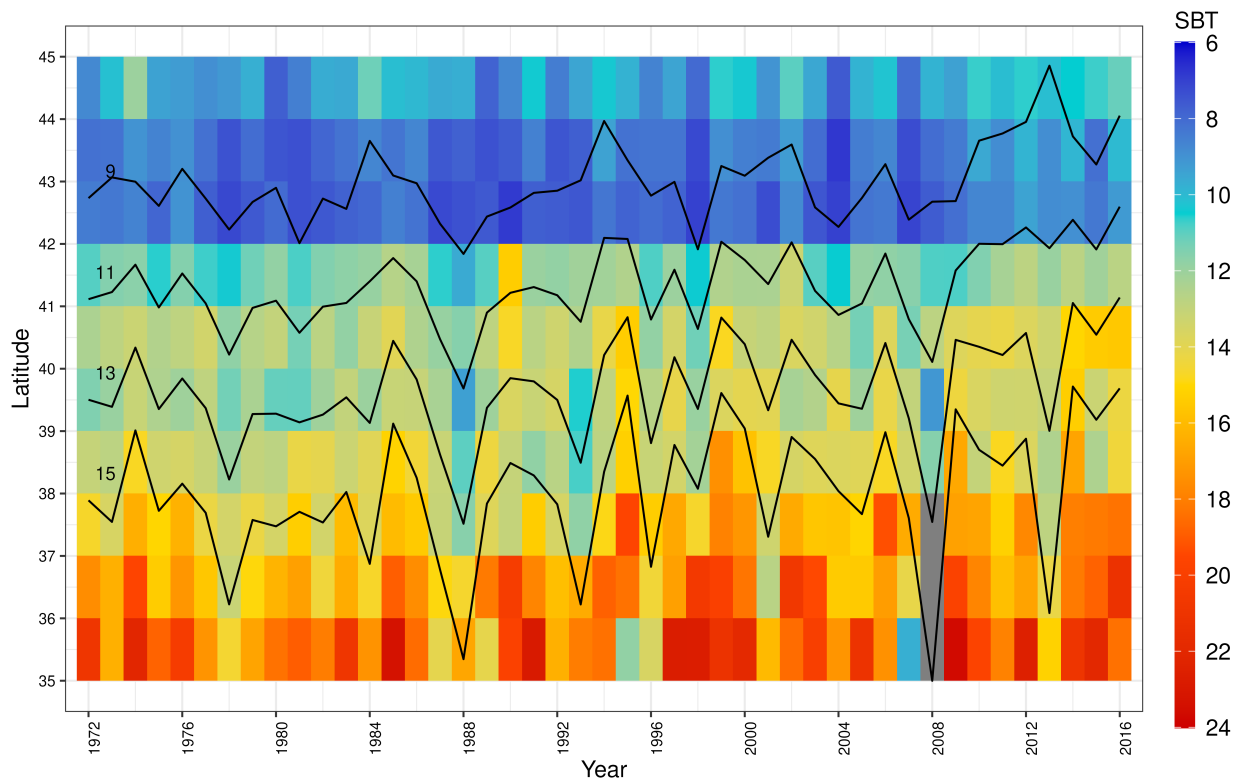


Figure 4: Sea bottom temperatures (SBT) recorded *in situ* by trawl surveys by patch and year, calculated as means of haul-level observations. Grey boxes indicate data gaps. Solid black lines represent isotherms. Their positions were calculated by fitting a Bayesian linear regression with Gaussian errors of temperature on latitude in each year and calculating the median estimated latitudinal position of each degree Celcius isotherm value.

408 ment of new offspring. Temperature-dependent mortality had a similar optimum (14.7 – 14.9
409 °C) but a greater width (4.23 – 5.73 °C) that implied substantially less sensitivity of mortality to
410 differences in temperature. By contrast, movement had a higher optimal temperature (16.4 – 20.4
411 °C) and a narrow width (1.03 – 1.28 °C), suggesting adults moved towards warmer waters than
412 were optimal for recruitment of offspring. The temperature-dependent mortality model and the
413 null model estimated intermediate values for the between-patch diffusion rate (0.03 – 0.17 and
414 0.06 – 0.21); and the temperature-dependent recruitment model estimated a much lower adult
415 diffusion rate (0.0006 – 0.02).

416 The temperature-dependent recruitment forecast, the temperature-dependent mortality fore-
417 cast, and the persistence forecast most often had greater skill (lower RMSE) and less bias out-
418 of-sample than the other models tested (Fig. 5, Supp. Fig. 8). Both of these DRMs notably
419 out-performed the persistence forecast at the warm range edge, where the persistence forecast
420 substantially over-predicted the edge latitude (Fig. 6). The GAM and other two DRM configura-
421 tions (a temperature effect on movement, or no temperature effect) performed worse across the
422 considered metrics, with less skill and greater bias. For the temperature-dependent recruitment
423 DRM, every observed range metric fell within the 95% HPDI in every year (Fig. 6). By contrast,
424 the GAM over-predicted the range size of summer flounder, estimating the warm edge further
425 south and the cold edge much further north than they were found in the survey (Fig. 6). The ob-
426 served spatiotemporal distribution of summer flounder in the survey from 2007-2016 was highly
427 concentrated between 37-40°N, which was better captured by the persistence and DRM forecasts
428 (Fig. 3).

429 3 Discussion

430 Integrating greater biological process and mechanism into forecasts of species responses to cli-
431 mate change and variation has long been a goal (Pagel & Schurr, 2012; Urban et al., 2016). Here,
432 we showed that dynamic range models with climate-dependent demographic rates outperformed
433 a statistical SDM and a persistence forecast in near-term forecasting of range dynamics during a
434 10-year interval of environmental variability. These results provided evidence that rates of pop-

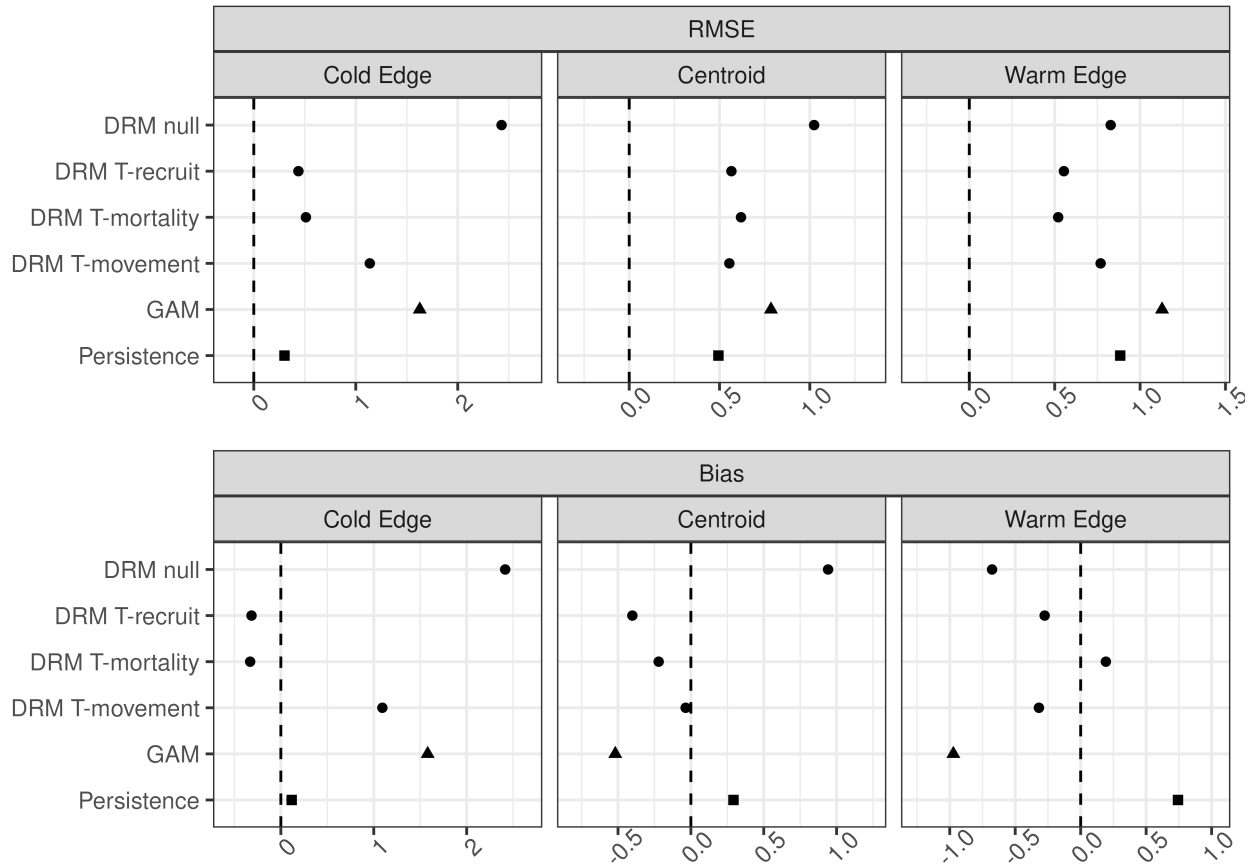


Figure 5: Skill of DRMs, GAM, and a persistence forecast at predicting summer flounder range dynamics out-of-sample from 2007-2016 measured as root mean square error (RMSE) and bias. The DRMs included no temperature effect (null) or a temperature effect on recruitment (T-recruit), mortality (T-mortality), or movement (T-movement). We measured ranged dynamics with three metrics: the warm and cold range edge positions and the centroid (abundance-weighted latitudinal average) every year. RMSE measures how close the predictions were to the observed values; lower RMSE values indicate greater accuracy. Bias measures whether the predictions were consistently too far north (positive bias) or too far south (negative bias); values closer to zero (indicated by the vertical dashed line) indicate less bias. Note that x-axis scales vary by panel.

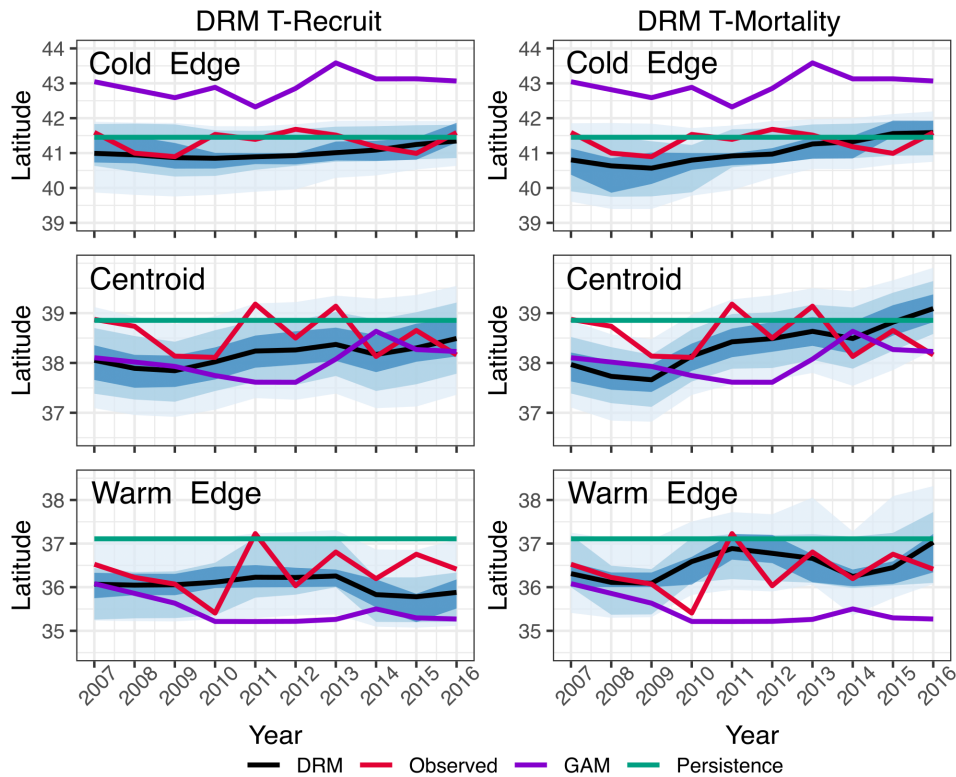


Figure 6: Observed range dynamics of summer flounder (red line) in the study domain (Fig. 2) during the testing decade (2007-2016) and range dynamics forecasted by the temperature-dependent recruitment (left) and temperature-dependent mortality (right) DRMs and by the GAM and persistence forecasts. Latitudinal positions of the cold edge (top row), range centroid (middle row), and warm edge of the population (bottom row) are shown. Shaded blue regions represent HPDIs (0.5, 0.8, and 0.95) of the DRM forecast.

435 ulation growth, dispersal, and reproduction are important for understanding species responses
436 to a changing climate, especially in the common scenario where species are not in equilibrium
437 with the climate (Guisan & Thuiller, 2005). Because of their Bayesian structure, the DRMs also
438 allowed the quantification and communication of uncertainty around forecasted state variables
439 like geographic position.

440 By testing alternative mechanistic models, our approach further provided evidence that range
441 shifts in summer flounder can be explained by temperature-dependent recruitment or mortal-
442 ity. Temperature-dependent recruitment may drive northward shifts as habitats warm further
443 north and become thermally suitable for larvae and small juveniles. Indeed, a more rapid
444 northward shift in small juvenile summer flounder than in adults has been reported (Perretti
445 & Thorson, 2019). Alternatively, increasing rates of survival at and beyond northern range edges
446 can also drive a northern shift in the density of the species, as suggested by the temperature-
447 dependent mortality model. Previous research suggested that summer flounder mortality is
448 linked to oceanographic conditions, though that study did not try to explain the northward ge-
449 ographic shift in summer flounder distributions (O'Leary et al., 2019). In addition, our results
450 lend support to the hypothesis that adult fish prefer and move towards higher temperatures
451 than are optimal for larvae and juveniles. This ontogenetic difference is consistent with patterns
452 across fishes suggesting that adult high temperature limits are higher than for larvae (Dahlke
453 et al., 2020), though inconsistent with generally lower temperature preferences in larger than in
454 smaller fishes (Lafrance et al., 2005). More broadly, our application of DRMs provides a model for
455 moving research on geographic range shifts towards demographic and ecological mechanisms.
456 The explicit demography in the DRMs allows them to be theoretically extended to include other
457 mechanisms, including species interactions (Urban et al., 2016).

458 The persistence forecast—i.e., the prediction that future conditions will be identical to the
459 final year of available data—performed relatively well in our analysis. This result arose because
460 the geographic range of summer flounder was remarkably stable during the testing decade de-
461 spite marked environmental variability, and was unexpected given widespread observations of
462 temperature-related range shifts in marine fishes in this region (Fredston et al., 2021; Fredston-

463 Hermann et al., 2020; Mills et al., 2024; Pinsky et al., 2013). However, temporal autocorrelation
464 in biological systems (often termed “ecological memory”) is common and often used to inform
465 statistical models of near-term change (Ogle et al., 2015; Wolkovich et al., 2014). Indeed, the time
466 horizon of 1-10 years that we selected for its management relevance may be uniquely difficult
467 to predict, being longer than the daily-to-annual lead times of most near-term forecasting pro-
468 grams (Dietze et al., 2018) but shorter than mid- and end-century projections that ignore transient
469 population dynamics (Morley et al., 2018). Other studies at this time horizon have found that
470 persistence forecasts performed similarly to, or even better than, mechanistic models (Harris et
471 al., 2018; Ward et al., 2014). The time horizon chosen and the stable range dynamics exhibited by
472 summer flounder during an interval of significant warming likely also influenced the relatively
473 poor performance of the statistical SDM, though we note that extensive tuning and refinement
474 of the SDM was beyond the scope of our study (Brodie et al., 2022; Davies et al., 2023).

475 The DRM estimated some parameters that are difficult to observe, such the diffusion rate be-
476 tween habitat patches. This fact is both a feature, in that difficult-to-observe population processes
477 can be reconstructed, and a challenge, since these estimates are difficult to independently vali-
478 date. We emphasize that the primary purpose of this model is predictive, not providing precise
479 estimates of population parameters as would be done in a spatial stock assessment model (Punt,
480 2019). Indeed, as a consequence of designing a process-based model for prediction with multiple
481 options for temperature effects, there are subtle differences in the interpretation of certain model
482 parameters in the DRM (e.g., μ) depending on the model configuration (Equation (1) *versus*
483 Equation (7)). This distinction matters because the performance of a primarily predictive model
484 can only really be judged relative to a benchmark such as an alternative model, as we did here.
485 In contrast, an inference-focused model must demonstrate reliable identification of individual es-
486 timated parameters, which we have not rigorously explored here (Tredennick et al., 2021). There
487 is no guarantee that the model or parameter values that maximize predictive skill are the same
488 as those with the greatest inferential power.

489 Dynamic range models that represent biological processes can be extended to a wide range of
490 taxa and systems that are underrepresented in the literature on forecasting biodiversity responses

491 to global change (Urban et al., 2022; Zurell et al., 2022). One advantage of the DRM approach
492 is that, like other mechanistic models, it can in theory capture any ecological process for which
493 one can write down an equation hypothesizing its effect on a population parameter (Pagel &
494 Schurr, 2012). Another advantage is that DRMs are conducive to best practices in informing en-
495 vironmental decision-making, such as mechanistic representation of causal linkages, selection of
496 model structure for management relevance, measurement of forecast skill with decision-relevant
497 metrics, and quantification of uncertainty (Bodner et al., 2021; Mason et al., 2023; Schmolke et al.,
498 2010; Schuwirth et al., 2019). We tested mechanisms of temperature dependence and fishing for
499 a single species as a case study. Future work can test the performance of models incorporating
500 temperature effects on multiple life history processes; incorporate new processes such as species
501 interactions, density dependence, or local adaptation; and test DRM approaches against more
502 species with different life histories. Methodological investigations of dynamic range modeling
503 are also needed, including the effect of spatial and temporal scale and extent on projections, and
504 incorporating multiple observational data streams. Both kinds of research would be facilitated
505 by easy-to-use computational and statistical tools for creating, fitting, and evaluating DRMs. In
506 addition, for the summer flounder DRM to be operational as a future (rather than retrospective)
507 forecasting system, additional work would be needed to incorporate future temperature projec-
508 tions (e.g., Koul et al., 2024). Given the limited use to date of mechanistic models that are both
509 validated against historical observations and ready to forecast species on the move, we hope that
510 the results here motivate further investment in this promising new field.

511

Data and Code Accessibility Statement

512 An de-identified version of the GitHub repository has been generated via Anonymous Github
513 (<https://anonymous.4open.science>) and is available at: [https://anonymous.4open.science/r/
514 mid_atlantic_forecasts-318E/](https://anonymous.4open.science/r/mid_atlantic_forecasts-318E/).

Acknowledgments

515

516 Removed for double-anonymous review.

Author Contribution Statement

517

518 Removed for double-anonymous review.

References

519

- 520 Bodner, K., Rauen Firkowski, C., Bennett, J. R., Brookson, C., Dietze, M., Green, S., Hughes, J.,
521 Kerr, J., Kunegel-Lion, M., Leroux, S. J., McIntire, E., Molnár, P. K., Simpkins, C., Tekwa,
522 E., Watts, A., & Fortin, M.-J. (2021). Bridging the divide between ecological forecasts and
523 environmental decision making [eprint: <https://onlinelibrary.wiley.com/doi/pdf/10.1002/ecs2.3869>].
524 *Ecosphere*, 12(12), e03869. <https://doi.org/10.1002/ecs2.3869>
- 525 Briscoe, N. J., Elith, J., Salguero-Gómez, R., Lahoz-Monfort, J. J., Camac, J. S., Giljohann, K. M.,
526 Holden, M. H., Hradsky, B. A., Kearney, M. R., McMahon, S. M., Phillips, B. L., Regan,
527 T. J., Rhodes, J. R., Vesk, P. A., Wintle, B. A., Yen, J. D. L., & Guillera-Arroita, G. (2019).
528 Forecasting species range dynamics with process-explicit models: Matching methods to
529 applications. *Ecology Letters*, 22(11), 1940–1956. <https://doi.org/10.1111/ele.13348>
- 530 Brodie, S., Smith, J. A., Muhling, B. A., Barnett, L. A. K., Carroll, G., Fiedler, P., Bograd, S. J.,
531 Hazen, E. L., Jacox, M. G., Andrews, K. S., Barnes, C. L., Crozier, L. G., Fiechter, J., Fred-
532 ston, A., Haltuch, M. A., Harvey, C. J., Holmes, E., Karp, M. A., Liu, O. R., . . . Kaplan, I. C.
533 (2022). Recommendations for quantifying and reducing uncertainty in climate projections
534 of species distributions [eprint: <https://onlinelibrary.wiley.com/doi/pdf/10.1111/gcb.16371>].
535 *Global Change Biology*, 28(22), 6586–6601. <https://doi.org/10.1111/gcb.16371>
- 536 Cabral, J. S., Valente, L., & Hartig, F. (2017). Mechanistic simulation models in macroecology and
537 biogeography: State-of-art and prospects [eprint: <https://onlinelibrary.wiley.com/doi/pdf/10.1111/eco>
538 *Ecography*, 40(2), 267–280. <https://doi.org/10.1111/ecog.02480>

539 Dahlke, F. T., Wohlrab, S., Butzin, M., & Pörtner, H.-O. (2020). Thermal bottlenecks in the life cycle
540 define climate vulnerability of fish [Publisher: American Association for the Advancement
541 of Science Section: Research Article]. *Science*, 369(6499), 65–70. [https://doi.org/10.1126/
542 science.aaz3658](https://doi.org/10.1126/science.aaz3658)

543 Davies, S. C., Thompson, P. L., Gomez, C., Nephin, J., Knudby, A., Park, A. E., Friesen, S. K.,
544 Pollock, L. J., Rubidge, E. M., Anderson, S. C., Iacarella, J. C., Lyons, D. A., MacDon-
545 ald, A., McMillan, A., Ward, E. J., Holdsworth, A. M., Swart, N., Price, J., & Hunter,
546 K. L. (2023). Addressing uncertainty when projecting marine species' distributions under
547 climate change [eprint: <https://onlinelibrary.wiley.com/doi/pdf/10.1111/ecog.06731>].
548 *Ecography*, 2023(11), e06731. <https://doi.org/10.1111/ecog.06731>

549 Davis, A. J., Jenkinson, L. S., Lawton, J. H., Shorrocks, B., & Wood, S. (1998). Making mistakes
550 when predicting shifts in species range in response to global warming. *Nature*, 391(6669),
551 783–786. <https://doi.org/10.1038/35842>

552 Dietze, M. C., Fox, A., Beck-Johnson, L. M., Betancourt, J. L., Hooten, M. B., Jarnevich, C. S.,
553 Keitt, T. H., Kenney, M. A., Laney, C. M., Larsen, L. G., Loescher, H. W., Lunch, C. K.,
554 Pijanowski, B. C., Randerson, J. T., Read, E. K., Tredennick, A. T., Vargas, R., Weathers,
555 K. C., & White, E. P. (2018). Iterative near-term ecological forecasting: Needs, opportu-
556 nities, and challenges. *Proceedings of the National Academy of Sciences*, 115(7), 1424–1432.
557 <https://doi.org/10.1073/pnas.1710231115>

558 Ehrlén, J., & Morris, W. F. (2015). Predicting changes in the distribution and abundance of species
559 under environmental change. *Ecology Letters*, 18(3), 303–314. [https://doi.org/10.1111/
560 ele.12410](https://doi.org/10.1111/ele.12410)

561 Elith, J., & Leathwick, J. R. (2009). Species Distribution Models: Ecological Explanation and Pre-
562 diction Across Space and Time. *Annual Review of Ecology, Evolution, and Systematics*, 40(1),
563 677–697. <https://doi.org/10.1146/annurev.ecolsys.110308.120159>

564 Evans, M. E. K., Merow, C., Record, S., McMahon, S. M., & Enquist, B. J. (2016). Towards Process-
565 based Range Modeling of Many Species. *Trends in Ecology & Evolution*, 31(11), 860–871.
566 <https://doi.org/10.1016/j.tree.2016.08.005>

567 Forrest, D., Stuart, M., & Pinsky, M. L. (2020). Scripts and data for OceanAdapt website to
568 visualize shifts in marine animal distributions: Update 2020. [https://doi.org/10.5281/
569 zenodo.3885625](https://doi.org/10.5281/zenodo.3885625)

570 Fredston, A., Pinsky, M., Selden, R. L., Szuwalski, C., Thorson, J. T., Gaines, S. D., & Halpern,
571 B. S. (2021). Range edges of North American marine species are tracking temperature over
572 decades [eprint: <https://onlinelibrary.wiley.com/doi/pdf/10.1111/gcb.15614>]. *Global Change
573 Biology*, 27(13), 3145–3156. <https://doi.org/10.1111/gcb.15614>

574 Fredston-Hermann, A., Selden, R., Pinsky, M., Gaines, S. D., & Halpern, B. S. (2020). Cold
575 range edges of marine fishes track climate change better than warm edges [eprint:
576 <https://onlinelibrary.wiley.com/doi/pdf/10.1111/gcb.15035>]. *Global Change Biology*, 26(5),
577 2908–2922. <https://doi.org/10.1111/gcb.15035>

578 Gabry, J., Češnovar, R., Johnson, A., & Bröder, S. (2024). *Cmdstanr: R Interface to 'CmdStan'*.

579 Guisan, A., & Thuiller, W. (2005). Predicting species distribution: Offering more than simple
580 habitat models [WOS:000231224600011]. *Ecology Letters*, 8(9), 993–1009. [https://doi.org/
581 10.1111/j.1461-0248.2005.00792.x](https://doi.org/10.1111/j.1461-0248.2005.00792.x)

582 Harris, D. J., Taylor, S. D., & White, E. P. (2018). Forecasting biodiversity in breeding birds using
583 best practices. *PeerJ*, 6. <https://doi.org/10.7717/peerj.4278>

584 Hoey, J. A., Fodrie, F. J., Walker, Q. A., Hilton, E. J., Kellison, G. T., Targett, T. E., Taylor, J. C., Able,
585 K. W., & Pinsky, M. L. (2020). Using multiple natural tags provides evidence for extensive
586 larval dispersal across space and through time in summer flounder [Publisher: John Wiley
587 & Sons, Ltd]. *Molecular Ecology*, 29(8), 1421–1435. <https://doi.org/10.1111/mec.15414>

588 Hoey, J. A., & Pinsky, M. L. (2018). Genomic signatures of environmental selection despite near-
589 panmixia in summer flounder [Publisher: John Wiley & Sons, Ltd]. *Evolutionary Applica-
590 tions*, 11(9), 1732–1747. <https://doi.org/10.1111/eva.12676>

591 Houde, E. D. (2008). Emerging from Hjort's Shadow. *Journal of Northwest Atlantic Fishery Science*,
592 41, 53–70. <https://doi.org/10.2960/J.v41.m634>

- 593 Jarnevich, C. S., Stohlgren, T. J., Kumar, S., Morisette, J. T., & Holcombe, T. R. (2015). Caveats for
594 correlative species distribution modeling. *Ecological Informatics*, 29, 6–15. [https://doi.org/
595 10.1016/j.ecoinf.2015.06.007](https://doi.org/10.1016/j.ecoinf.2015.06.007)
- 596 Johnson, K. F., Councill, E., Thorson, J. T., Brooks, E., Methot, R. D., & Punt, A. E. (2016). Can
597 autocorrelated recruitment be estimated using integrated assessment models and how
598 does it affect population forecasts? *Fisheries Research*, 183, 222–232. [https://doi.org/10.
599 1016/j.fishres.2016.06.004](https://doi.org/10.1016/j.fishres.2016.06.004)
- 600 Kearney, M., & Porter, W. (2009). Mechanistic niche modelling: Combining physiological and
601 spatial data to predict species' ranges. *Ecology Letters*, 12(4), 334–350. [https://doi.org/10.
602 1111/j.1461-0248.2008.01277.x](https://doi.org/10.1111/j.1461-0248.2008.01277.x)
- 603 Keefe, M., & Able, K. W. (1993). Patterns of metamorphosis in summer flounder, *Paralichthys den-*
604 *tatus* [eprint: <https://onlinelibrary.wiley.com/doi/pdf/10.1111/j.1095-8649.1993.tb00380.x>].
605 *Journal of Fish Biology*, 42(5), 713–728. <https://doi.org/10.1111/j.1095-8649.1993.tb00380.x>
- 606 Koul, V., Ross, A. C., Stock, C., Zhang, L., Delworth, T., & Wittenberg, A. (2024). A Predicted
607 Pause in the Rapid Warming of the Northwest Atlantic Shelf in the Coming Decade
608 [eprint: <https://onlinelibrary.wiley.com/doi/pdf/10.1029/2024GL110946>]. *Geophysical Re-*
609 *search Letters*, 51(17), e2024GL110946. <https://doi.org/10.1029/2024GL110946>
- 610 Lafrance, P., Castonguay, M., Chabot, D., & Audet, C. (2005). Ontogenetic changes in temperature
611 preference of Atlantic cod [eprint: [https://onlinelibrary.wiley.com/doi/pdf/10.1111/j.0022-
612 1112.2005.00623.x](https://onlinelibrary.wiley.com/doi/pdf/10.1111/j.0022-1112.2005.00623.x)]. *Journal of Fish Biology*, 66(2), 553–567. [https://doi.org/10.1111/j.0022-
613 1112.2005.00623.x](https://doi.org/10.1111/j.0022-1112.2005.00623.x)
- 614 Laubmeier, A. N., Cazelles, B., Cuddington, K., Erickson, K. D., Fortin, M.-J., Ogle, K., Wikle,
615 C. K., Zhu, K., & Zipkin, E. F. (2020). Ecological Dynamics: Integrating Empirical, Statis-
616 tical, and Analytical Methods. *Trends in Ecology & Evolution*. [https://doi.org/10.1016/j.
617 tree.2020.08.006](https://doi.org/10.1016/j.tree.2020.08.006)
- 618 Le Squin, A., Boulangeat, I., & Gravel, D. (2021). Climate-induced variation in the demography
619 of 14 tree species is not sufficient to explain their distribution in eastern North America

620
621
622
623
624
625
626
627
628
629
630
631
632
633
634
635
636
637
638
639
640
641
642
643
644
645
646

[eprint: <https://onlinelibrary.wiley.com/doi/pdf/10.1111/geb.13209>]. *Global Ecology and Biogeography*, 30(2), 352–369. <https://doi.org/10.1111/geb.13209>

Lee-Yaw, J. A., L. McCune, J., Pironon, S., & N. Sheth, S. (2022). Species distribution models rarely predict the biology of real populations [eprint: <https://onlinelibrary.wiley.com/doi/pdf/10.1111/ecog.05877>]. *Ecography*, 2022(6), e05877. <https://doi.org/10.1111/ecog.05877>

Lux, F. E., & Nichy, F. E. (1981). *Movements of tagged summer flounder, Paralichthys dentatus, off southern New England* (NOAA Technical Report No. NMFS SSRF-752). National Oceanic and Atmospheric Administration.

Mason, J. G., Weisberg, S. J., Morano, J. L., Bell, R. J., Fitchett, M., Griffis, R. B., Hazen, E. L., Heyman, W. D., Holsman, K., Kleisner, K. M., Westfall, K., Conrad, M. K., Daly, M., Golden, A. S., Harvey, C. J., Kerr, L. A., Kirchner, G., Levine, A., Lewison, R. L., ... Stram, D. L. (2023). Linking knowledge and action for climate-ready fisheries: Emerging best practices across the US. *Marine Policy*, 155, 105758. <https://doi.org/10.1016/j.marpol.2023.105758>

Maureaud, A., Abrantes, J. P., Kitchel, Z., Mannocci, L., Pinsky, M., Fredston, A., Beukhof, E., Forrest, D., Frelat, R., Palomares, D., Pecuchet, L., Thorson, J., Denderen, D. v., & Merigot, B. (2023, January). FishGlob_data: An integrated database of fish biodiversity sampled with scientific bottom-trawl surveys. <https://doi.org/10.31219/osf.io/2bcjw>

McCoy, M. W., & Gillooly, J. F. (2008). Predicting natural mortality rates of plants and animals [eprint: <https://onlinelibrary.wiley.com/doi/pdf/10.1111/j.1461-0248.2008.01190.x>]. *Ecology Letters*, 11(7), 710–716. <https://doi.org/10.1111/j.1461-0248.2008.01190.x>

Mills, K. E., Kemberling, A., Kerr, L. A., Lucey, S. M., McBride, R. S., Nye, J. A., Pershing, A. J., Barajas, M., & Lovas, C. S. (2024). Multispecies population-scale emergence of climate change signals in an ocean warming hotspot. *ICES Journal of Marine Science*, fsad208. <https://doi.org/10.1093/icesjms/fsad208>

Morales, J. M., Moorcroft, P. R., Matthiopoulos, J., Frair, J. L., Kie, J. G., Powell, R. A., Merrill, E. H., & Haydon, D. T. (2010). Building the bridge between animal movement and popula-

647 tion dynamics. *Philosophical Transactions of the Royal Society B: Biological Sciences*, 365(1550),
648 2289–2301. <https://doi.org/10.1098/rstb.2010.0082>

649 Morley, J. W., Selden, R. L., Latour, R. J., Frölicher, T. L., Seagraves, R. J., & Pinsky, M. L. (2018).
650 Projecting shifts in thermal habitat for 686 species on the North American continental
651 shelf [Publisher: Public Library of Science]. *PLOS ONE*, 13(5), e0196127. [https://doi.org/](https://doi.org/10.1371/journal.pone.0196127)
652 [10.1371/journal.pone.0196127](https://doi.org/10.1371/journal.pone.0196127)

653 Mouquet, N., Lagadeuc, Y., Devictor, V., Doyen, L., Duputié, A., Eveillard, D., Faure, D., Garnier,
654 E., Gimenez, O., Huneman, P., Jabot, F., Jarne, P., Joly, D., Julliard, R., Kéfi, S., Kergoat,
655 G. J., Lavorel, S., Le Gall, L., Meslin, L., ... Loreau, M. (2015). Predictive ecology in a
656 changing world. *Journal of Applied Ecology*, 52(5), 1293–1310. [https://doi.org/10.1111/](https://doi.org/10.1111/1365-2664.12482)
657 [1365-2664.12482](https://doi.org/10.1111/1365-2664.12482)

658 Munch, S. B., & Salinas, S. (2009). Latitudinal variation in lifespan within species is explained
659 by the metabolic theory of ecology [Publisher: National Academy of Sciences Section:
660 Biological Sciences]. *Proceedings of the National Academy of Sciences*, 106(33), 13860–13864.
661 <https://doi.org/10.1073/pnas.0900300106>

662 NEFSC. (2019). *66th Northeast Regional Stock Assessment Workshop (66th SAW) Assessment Report*
663 (tech. rep. No. Northeast Fish Sci Cent Ref Doc. 19-08). Northeast Fisheries Science Center.

664 Ogle, K., Barber, J. J., Barron-Gafford, G. A., Bentley, L. P., Young, J. M., Huxman, T. E., Loik,
665 M. E., & Tissue, D. T. (2015). Quantifying ecological memory in plant and ecosystem
666 processes [eprint: <https://onlinelibrary.wiley.com/doi/pdf/10.1111/ele.12399>]. *Ecology*
667 *Letters*, 18(3), 221–235. <https://doi.org/10.1111/ele.12399>

668 O’Leary, C. A., Miller, T. J., Thorson, J. T., & Nye, J. A. (2019). Understanding historical sum-
669 mer flounder (*Paralichthys dentatus*) abundance patterns through the incorporation of
670 oceanography-dependent vital rates in Bayesian hierarchical models [Publisher: NRC Re-
671 search Press]. *Canadian Journal of Fisheries and Aquatic Sciences*, 76(8), 1275–1294. <https://doi.org/10.1139/cjfas-2018-0092>

673 Osada, Y., Kuriyama, T., Asada, M., Yokomizo, H., & Miyashita, T. (2019). Estimating range ex-
674 pansion of wildlife in heterogeneous landscapes: A spatially explicit state-space matrix

675
676
677
678
679
680
681
682
683
684
685
686
687
688
689
690
691
692
693
694
695
696
697
698
699
700

model coupled with an improved numerical integration technique [eprint: <https://onlinelibrary.wiley.com/doi/10.1002/ece3.4739>
Ecology and Evolution, 9(1), 318–327. <https://doi.org/10.1002/ece3.4739>

Packer, D. B., Griesbach, S. J., Berrien, P. L., Zetlin, C. A., Johnson, D. L., & Morse, W. W. (1999, September). *Essential Fish Habitat Source Document: Summer flounder, *Paralichthys dentatus*, Life History and Habitat Characteristics* (NOAA Technical Memorandum No. NMFS-NE-151). Northeast Fisheries Science Center. Woods Hole, Massachusetts.

Pagel, J., & Schurr, F. M. (2012). Forecasting species ranges by statistical estimation of ecological niches and spatial population dynamics. *Global Ecology and Biogeography*, 21(2), 293–304. <https://doi.org/10.1111/j.1466-8238.2011.00663.x>

Pappalardo, P., Pringle, J. M., Wares, J. P., & Byers, J. E. (2015). The location, strength, and mechanisms behind marine biogeographic boundaries of the east coast of North America. *Ecography*, 38(7), 722–731. <https://doi.org/10.1111/ecog.01135>

Parmesan, C., & Yohe, G. (2003). A globally coherent fingerprint of climate change impacts across natural systems. *Nature*, 421(6918), 37–42. <https://doi.org/10.1038/nature01286>

Pearson, R. G., & Dawson, T. P. (2003). Predicting the impacts of climate change on the distribution of species: Are bioclimate envelope models useful? [eprint: <https://onlinelibrary.wiley.com/doi/pdf/10.1046/j.1466-822X.2003.00042.x>]. *Global Ecology and Biogeography*, 12(5), 361–371. <https://doi.org/10.1046/j.1466-822X.2003.00042.x>

Pecl, G. T., Araújo, M. B., Bell, J. D., Blanchard, J., Bonebrake, T. C., Chen, I.-C., Clark, T. D., Colwell, R. K., Danielsen, F., Evengård, B., Falconi, L., Ferrier, S., Frusher, S., Garcia, R. A., Griffis, R. B., Hobday, A. J., Janion-Scheepers, C., Jarzyna, M. A., Jennings, S., . . . Williams, S. E. (2017). Biodiversity redistribution under climate change: Impacts on ecosystems and human well-being. *Science*, 355(6332), eaai9214. <https://doi.org/10.1126/science.aai9214>

Perretti, C. T., & Thorson, J. T. (2019). Spatio-temporal dynamics of summer flounder (*Paralichthys dentatus*) on the Northeast US shelf. *Fisheries Research*, 215, 62–68. <https://doi.org/10.1016/j.fishres.2019.03.006>

- 701 Pinsky, M. L., Selden, R. L., & Kitchel, Z. J. (2020). Climate-Driven Shifts in Marine Species
702 Ranges: Scaling from Organisms to Communities. *Annual Review of Marine Science*, 12(1).
703 <https://doi.org/10.1146/annurev-marine-010419-010916>
- 704 Pinsky, M. L., Worm, B., Fogarty, M. J., Sarmiento, J. L., & Levin, S. A. (2013). Marine taxa track
705 local climate velocities. *Science*, 341(6151), 1239–1242.
- 706 Potts, J. M., & Elith, J. (2006). Comparing species abundance models. *Ecological Modelling*, 199(2),
707 153–163. <https://doi.org/10.1016/j.ecolmodel.2006.05.025>
- 708 Potts, J. R., & Schlägel, U. E. (2020). Parametrizing diffusion-taxis equations from animal move-
709 ment trajectories using step selection analysis [eprint: [https://besjournals.onlinelibrary.wiley.com/doi/10.1111/](https://besjournals.onlinelibrary.wiley.com/doi/10.1111/210X.13406)
710 [210X.13406](https://doi.org/10.1111/210X.13406)]. *Methods in Ecology and Evolution*, 11(9), 1092–1105. [https://doi.org/10.1111/](https://doi.org/10.1111/2041-210X.13406)
711 [2041-210X.13406](https://doi.org/10.1111/2041-210X.13406)
- 712 Preisler, H. K., Ager, A. A., & Wisdom, M. J. (2013). Analyzing animal movement patterns using
713 potential functions [eprint: [https://esajournals.onlinelibrary.wiley.com/doi/pdf/10.1890/ES12-](https://esajournals.onlinelibrary.wiley.com/doi/pdf/10.1890/ES12-00286.1)
714 [00286.1](https://doi.org/10.1890/ES12-00286.1)]. *Ecosphere*, 4(3), art32. <https://doi.org/10.1890/ES12-00286.1>
- 715 Punt, A. E. (2019). Spatial stock assessment methods: A viewpoint on current issues and assump-
716 tions. *Fisheries Research*, 213, 132–143. <https://doi.org/10.1016/j.fishres.2019.01.014>
- 717 Rubenstein, M. A., Weiskopf, S. R., Bertrand, R., Carter, S. L., Comte, L., Eaton, M. J., Johnson,
718 C. G., Lenoir, J., Lynch, A. J., Miller, B. W., Morelli, T. L., Rodriguez, M. A., Terando,
719 A., & Thompson, L. M. (2023). Climate change and the global redistribution of biodiver-
720 sity: Substantial variation in empirical support for expected range shifts. *Environmental*
721 *Evidence*, 12(1), 7. <https://doi.org/10.1186/s13750-023-00296-0>
- 722 Scheffers, B. R., Meester, L. D., Bridge, T. C. L., Hoffmann, A. A., Pandolfi, J. M., Corlett, R. T.,
723 Butchart, S. H. M., Pearce-Kelly, P., Kovacs, K. M., Dudgeon, D., Pacifici, M., Rondinini,
724 C., Foden, W. B., Martin, T. G., Mora, C., Bickford, D., & Watson, J. E. M. (2016). The broad
725 footprint of climate change from genes to biomes to people. *Science*, 354(6313), aaf7671.
726 <https://doi.org/10.1126/science.aaf7671>

727 Schmolke, A., Thorbek, P., DeAngelis, D. L., & Grimm, V. (2010). Ecological models supporting
728 environmental decision making: A strategy for the future. *Trends in Ecology & Evolution*,
729 25(8), 479–486. <https://doi.org/10.1016/j.tree.2010.05.001>

730 Schuwirth, N., Borgwardt, F., Domisch, S., Friedrichs, M., Kattwinkel, M., Kneis, D., Kuemmerlen,
731 M., Langhans, S. D., Martínez-López, J., & Vermeiren, P. (2019). How to make ecological
732 models useful for environmental management. *Ecological Modelling*, 411, 108784. <https://doi.org/10.1016/j.ecolmodel.2019.108784>

734 Smith, T. D. (2002). The Woods Hole bottom-trawl resource survey: Development of fisheries-
735 independent multispecies monitoring [Publisher: ICES]. <https://doi.org/10.17895/ICES.PUB.8888>

736

737 Stan Development Team. (2021). RStan: The R interface to Stan.

738 Sunday, J. M., Bates, A. E., & Dulvy, N. K. (2012). Thermal tolerance and the global redistribution
739 of animals. *Nature Climate Change*, 2(9), 686–690. <https://doi.org/10.1038/nclimate1539>

740 Swearer, S. E., Treml, E. A., & Shima, J. S. (2019, August). A Review of Biophysical Models of
741 Marine Larval Dispersal. In S. Hawkins, A. Allcock, A. Bates, L. Firth, I. Smith, S. Swearer,
742 & P. Todd (Eds.), *Oceanography and Marine Biology* (1st ed., pp. 325–356). CRC Press. <https://doi.org/10.1201/9780429026379-7>

743

744 Terceiro, M. (2011). The summer flounder chronicles II: New science, new controversy, 2001–2010.
745 *Reviews in Fish Biology and Fisheries*, 21(4), 681–712. [https://doi.org/10.1007/s11160-011-](https://doi.org/10.1007/s11160-011-9207-9)
746 [9207-9](https://doi.org/10.1007/s11160-011-9207-9)

747 Thorson, J. T., Barbeaux, S. J., Goethel, D. R., Kearney, K. A., Laman, E. A., Nielsen, J. K., Siskey,
748 M. R., Siwicke, K., & Thompson, G. G. (2021). Estimating fine-scale movement rates and
749 habitat preferences using multiple data sources [eprint: <https://onlinelibrary.wiley.com/doi/pdf/10.1111/faf.12592>]
750 *Fish and Fisheries*, 22(6), 1359–1376. <https://doi.org/10.1111/faf.12592>

751 Thorson, J. T., Jensen, O. P., & Zipkin, E. F. (2014). How variable is recruitment for exploited ma-
752 rine fishes? A hierarchical model for testing life history theory [Publisher: NRC Research
753 Press]. *Canadian Journal of Fisheries and Aquatic Sciences*, 71(7), 973–983. <https://doi.org/10.1139/cjfas-2013-0645>

754

- 755 Tredennick, A. T., Hooker, G., Ellner, S. P., & Adler, P. B. (2021). A practical guide to selecting
756 models for exploration, inference, and prediction in ecology [eprint: <https://esajournals.onlinelibrary.wiley.com/doi/pdf/10.1002/ecy.3336>].
757 *Ecology*, 102(6), e03336. <https://doi.org/10.1002/ecy.3336>
- 758 Urban, M. C., Bocedi, G., Hendry, A. P., Mihoub, J.-B., Pe'er, G., Singer, A., Bridle, J. R., Crozier,
759 L. G., Meester, L. D., Godsoe, W., Gonzalez, A., Hellmann, J. J., Holt, R. D., Huth, A.,
760 Johst, K., Krug, C. B., Leadley, P. W., Palmer, S. C. F., Pantel, J. H., ... Travis, J. M. J.
761 (2016). Improving the forecast for biodiversity under climate change. *Science*, 353(6304),
762 aad8466. <https://doi.org/10.1126/science.aad8466>
- 763 Urban, M. C., Travis, J. M. J., Zurell, D., Thompson, P. L., Synes, N. W., Scarpa, A., Peres-Neto,
764 P. R., Malchow, A.-K., James, P. M. A., Gravel, D., De Meester, L., Brown, C., Bocedi,
765 G., Albert, C. H., Gonzalez, A., & Hendry, A. P. (2022). Coding for Life: Designing a
766 Platform for Projecting and Protecting Global Biodiversity. *BioScience*, 72(1), 91–104. <https://doi.org/10.1093/biosci/biab099>
767 <https://doi.org/10.1093/biosci/biab099>
- 768 Ward, E. J., Holmes, E. E., Thorson, J. T., & Collen, B. (2014). Complexity is costly: A meta-
769 analysis of parametric and non-parametric methods for short-term population forecast-
770 ing [eprint: <https://onlinelibrary.wiley.com/doi/pdf/10.1111/j.1600-0706.2014.00916.x>].
771 *Oikos*, 123(6), 652–661. <https://doi.org/10.1111/j.1600-0706.2014.00916.x>
- 772 Watson, J. R., Mitarai, S., Siegel, D. A., Caselle, J. E., Dong, C., & McWilliams, J. C. (2010). Realized
773 and potential larval connectivity in the Southern California Bight. *Marine Ecology Progress
774 Series*, 401, 31–48. <https://doi.org/10.3354/meps08376>
- 775 Wolkovich, E. M., Cook, B. I., McLauchlan, K. K., & Davies, T. J. (2014). Temporal ecology in
776 the Anthropocene [eprint: <https://onlinelibrary.wiley.com/doi/pdf/10.1111/ele.12353>].
777 *Ecology Letters*, 17(11), 1365–1379. <https://doi.org/10.1111/ele.12353>
- 778 Wood, S. N. (2017). *Generalized Additive Models: An Introduction with R* (2nd ed.). Chapman;
779 Hall/CRC.
- 780 Zurell, D. (2017). Integrating demography, dispersal and interspecific interactions into bird distri-
781 bution models [eprint: <https://onlinelibrary.wiley.com/doi/pdf/10.1111/jav.01225>]. *Jour-
782 nal of Avian Biology*, 48(12), 1505–1516. <https://doi.org/10.1111/jav.01225>

- 783 Zurell, D., König, C., Malchow, A.-K., Kapitza, S., Bocedi, G., Travis, J., & Fandos, G. (2022). Spa-
784 tially explicit models for decision-making in animal conservation and restoration [eprint:
785 <https://onlinelibrary.wiley.com/doi/pdf/10.1111/ecog.05787>]. *Ecography*, 2022(4). <https://doi.org/10.1111/ecog.05787>
786
- 787 Zurell, D., Thuiller, W., Pagel, J., Cabral, J. S., Münkemüller, T., Gravel, D., Dullinger, S., Nor-
788 mand, S., Schiffrers, K. H., Moore, K. A., & Zimmermann, N. E. (2016). Benchmarking
789 novel approaches for modelling species range dynamics. *Global Change Biology*, 22(8),
790 2651–2664. <https://doi.org/10.1111/gcb.13251>